

# Identifying Epigenetic Signature of Breast Cancer with Machine Learning

Maxim Vaysburd\*

\*Stuyvesant High School, New York, NY, USA

\*mvaysburd10@stuy.edu

## ABSTRACT

The research reported in this paper identifies the epigenetic biomarker (methylation beta pattern) of breast cancer. Many cancers are triggered by abnormal gene expression levels caused by aberrant methylation of CpG sites in the DNA. In order to develop early diagnostics of cancer-causing methylations and to develop a treatment, it is necessary to identify a few dozen key cancer-related CpG methylation sites out of the millions of locations in the DNA. This research used public TCGA dataset to train a TensorFlow machine learning model to classify breast cancer versus non-breast-cancer tissue samples, based on over 300,000 methylation beta values in each sample. L1 regularization was applied to identify the CpG methylation sites most important for accurate classification. It was hypothesized that CpG sites with the highest learned model weights correspond to DNA locations most relevant to breast cancer. A reduced model trained on methylation betas of just the 25 CpG sites having the highest weights in the full model (trained on methylation betas at over 300,000 CpG sites) has achieved over 94% accuracy on evaluation data, confirming that the identified 25 CpG sites are indeed a biomarker of breast cancer.

## Introduction

Methylation is the addition of methyl groups to nucleotides in the DNA molecule. The effects of methylation are particularly important at CpG sites, which are regions of DNA where a cytosine nucleotide is followed by a guanine nucleotide. When a cytosine nucleotide at a CpG site in a promoter region of DNA is methylated, the resulting effect is downregulation of the expression of the respective gene. Methylation can occur at millions of CpG sites throughout the DNA. The CpG sites can be both overmethylated and undermethylated compared to normal levels<sup>1,2</sup>.

Abnormalities in DNA methylation are important causes of development and progression of cancer<sup>1-6</sup>. Indeed, aberrations in methylation levels often appear well before the cancer develops, even while the cells still look completely normal under the microscope<sup>6,7</sup>.

In cancers, it is common that CpG sites are over-methylated at genes that make proteins promoting tumor suppressor genes<sup>3,6,8,9</sup>, DNA repair genes<sup>7,10</sup>, and genes that control cell cycle, differentiation, and apoptosis<sup>11</sup>. This results in silencing of tumor suppression and DNA repair, which contributes to development of cancer via an increased occurrence of unrepaired gene mutations and runaway cancer cells<sup>2</sup>. The silencing of tumor suppressor genes by abnormal over-methylation is in fact much more frequent than their inactivation by DNA mutations<sup>12</sup>.

At the same time, CpG sites in cancer are often under-methylated at oncogenes, which can cause tumors when overexpressed<sup>6</sup>. Genome-wide average methylation levels are also significantly lower in tumors than in healthy cells, and are still lower in metastatic cancer cells<sup>3,8,9</sup>.

The presence of both hypo- and hyper-methylation in cancer cells means that effective pharmaceutical treatments will have to be able to correct dangerous methylation levels in both directions: decrease methylation at CpG sites where abnormally high methylation is harmful, and increase at sites where abnormally low methylation is harmful. Methylation abnormalities are reversible<sup>3</sup>, and there are indeed pharmaceuticals approved by the FDA that can be used to reduce methylation levels genome-wide<sup>4,6,13-15</sup>. They are used to treat precancerous conditions and certain cancers caused by over-methylation of tumor suppressor genes. However, those medications have side effects and may cause other cancers by increasing expression of oncogenes and genes that promote cell invasiveness, and by causing general instability of the genome via broad upregulation of gene expressions<sup>14,16</sup>.

Several years ago, CRISPR technology was developed to correct genetic abnormalities at precise locations in the DNA<sup>17</sup>. It is plausible that in another several years a technology will be developed to correct epigenetic abnormalities at precisely specified CpG methylation sites. In order to be able to apply this technology for prevention and treatment of cancer, it will be necessary to know exactly which CpG methylation sites to correct, and in which direction to change the methylation, out of the hundreds of thousands of CpG sites in the DNA whose methylation can be measured with currently available sequencing technologies.

This research identifies the key CpG sites in the DNA whose methylation levels comprise the biomarker (epigenetic signature) of breast cancer, and which can be used to identify, with high accuracy, breast cancer tissue samples among tissue samples of various other types of cancer.

## Results and Discussion

This research has identified 25 CpG locations in the DNA whose methylation beta patterns are sufficient to classify breast cancer vs. non-breast-cancer solid tissue samples with a 94.6% accuracy using a machine learning classification model trained on methylation beta values at those 25 locations (Figure 4).

This represents only a modest drop from the 98.6% accuracy on evaluation data in the breast cancer vs. non-breast-cancer classification model trained on the full set of 323,179 CpG sites (Figure 3). The retention of most of the accuracy indicates that the methylation beta patterns at the identified 25 CpG sites are, indeed, a biomarker of breast cancer and can be used to distinguish it from other types of cancer with high accuracy.

Nine of the genes containing the identified 25 CpG sites ( TAF3, SFRP4, SBDS, PPP2R2A, RASSF4, MTA2, ZNF135, CDHR2, PACS2) turn out to be directly involved in the cell cycle and to regulate cell growth, differentiation, division, apoptosis, and tumor suppression (Table 1). These findings further confirm the significance of the CpG methylation sites identified by this research as an epigenetic biomarker of breast cancer.

Several of the genes containing the identified 25 CpG sites have unknown functions as of yet, and could turn out to regulate tumor-related activities as well. Their role in breast cancer is yet to be determined, and presents a direction for future research.

The mean methylation beta values for the 25 CpG sites, for the breast-cancer and non-breast-cancer solid tissue samples, are shown in Table 2.

The methodology applied in this research can be extended to identify epigenetic biomarkers for types of cancer other than breast cancer (the BRCA study in TCGA). Another direction for future research is to learn epigenetic biomarkers shared by multiple cancer types, by training a machine learning model to classify cancerous vs. normal tissues.

The knowledge of the epigenetic signature of breast cancer identified in this research is valuable in several ways: it can enable development of medications to correct abnormal methylation at precisely the CpG sites that control expression of genes involved in the development and progression of cancer, and it can also be used for early diagnostics and prevention of breast cancer, at the stage where analysis of tissue cells under the microscope (in biopsies) doesn't show any abnormalities, yet the epigenetic signature of cancer is already present.

## Materials and Methods

The research reported in this paper was performed using data in the public DNA methylation betas dataset<sup>18</sup> produced by The Cancer Genome Atlas Program<sup>19</sup>, containing tissue samples from 32 different types of cancer. The data has been retrieved from the public dataset `isb-cgc:TCGA_hg38_data_v0`, hosted by the Institute for Systems Biology - Cancer Genomics Cloud (ISB-CGC)<sup>20</sup> project on Google Cloud<sup>21</sup>. The data has been accessed via Google BigQuery<sup>22</sup>. Methylation betas for more than 400,000 CpG sites in 8,703 solid cancer tissue samples (identified by unique aliquot barcodes) were retrieved from the `TCGA_hg38_data_v0.DNA_Methylation` table.

A subset of samples and CpG probes were selected for use in the project, such that each included sample would contain methylation betas for the same set of CpG probes. This step reduced the size of the research dataset to 8,126 aliquots, with the same 323,179 probes included with each aliquot.

In the next step, training examples were constructed for the machine learning classification model, with each training example comprising a list of 323,179 methylation beta values for one aliquot, as the input features of the model. For each training example, the label was set to 1 for aliquots derived from BRCA (breast cancer study) tissue samples, and 0 for aliquots from all other included TCGA cancer studies. In order to prevent the classification model from being biased towards 1 or 0 values of the label, the same number of training examples were constructed for BRCA as for all other (non-BRCA) studies combined. Within the non-BRCA class (comprising training examples with the label 0), the same number of training examples were constructed from aliquots in each included non-BRCA study. The number of solid cancer tissue samples (aliquots) available for each cancer study in the TCGA dataset ranges from 763 for BRCA (breast cancer study) to 10 for OV. Altogether, training examples were generated using aliquots from the 22 TCGA studies having the highest number of available tissue samples.

In the following step, a classification model was trained using the `tf.estimator.DNNClassifier` class available in the TensorFlow<sup>23</sup> machine learning library. The classifier has been configured with one fully connected layer containing 128 hidden units, and two classes (1 or 0) corresponding to training examples as being either BRCA or non-BRCA. The Proximal Adagrad optimizer (available as the `tf.train.ProximalAdagradOptimizer` class in TensorFlow) was used to train the model with L1 regularization enabled. The regularization level was set to 0.005 to force the model to use as few input features as possible

without significantly hurting the accuracy of classification. The goal in using L1 regularization was to identify CpG sites in the genome whose methylation beta values are the most indispensable for the model for accurate classification of training examples. The model was trained using 80% of all training examples constructed in the previous step, with the remaining 20% of examples held out for the evaluation of results. Upon completion of 30,000 training steps, 98.7% of weights in the model's fully connected layer had the value of zero (Figure 1).

In the next step, the CpG sites (probe IDs) were sorted by the sums of absolute values of their weights in the classification model's fully connected layer (Figure 2), and the 25 CpG probe IDs with the highest model weights were selected.

A new classification model was then trained using the same 80% of training examples as in the original model but with each example constrained to include methylation betas of the selected top 25 probe IDs only (instead of the 323,179 betas used to train the first model). The same 20% of examples (constrained to the top 25 probe IDs) were used for the evaluation of the model. The training of the second model was configured with the same settings as in the first model, except that this time regularization was not applied. The purpose of the second model was to verify that the selected top 25 probes are indeed the key CpG sites comprising the biomarker of breast cancer.

Upon completion of model training, the data in the [isb-cgc:platform\\_reference.GDC\\_hg38\\_methylation\\_annotation](#) table in BigQuery was used to identify the genes containing the model-selected top 25 CpG sites. The GeneCards<sup>24</sup> and OMIM<sup>25</sup> databases were then used to look up the functions of those genes.

Finally, the average methylation beta values were computed for the selected top 25 CpG sites, for BRCA and non-BRCA tissue samples in TCGA.

## Data Availability

The Cancer Genome Atlas data analysed during the current study is available in the public BigQuery dataset repository [isb-cgc:TCGA\\_hg38\\_data\\_v0](#) in Google Cloud, at [https://bigquery.cloud.google.com/dataset/isb-cgc:TCGA\\_hg38\\_data\\_v0](https://bigquery.cloud.google.com/dataset/isb-cgc:TCGA_hg38_data_v0).

## References

1. Wei, J. *et al.* Discovery and validation of hypermethylated markers for colorectal cancer. *Dis. Markers* **2016**, 1–7, DOI: <https://doi.org/10.1155/2016/2192853> (2016).
2. Bernstein, C. & Bernstein, H. Epigenetic reduction of DNA Repair in progression to cancer. *Adv. DNA Repair* DOI: <https://doi.org/10.5772/60022> (2015).
3. Jones, P. & Baylin, S. The fundamental role of epigenetic events in cancer. *Nat. Rev. Genet.* **3(6)**, 415–428, DOI: <https://doi.org/10.1038/nrg816> (2002).
4. Baylin, S. B. & Jones, P. A. A decade of exploring the cancer epigenome — biological and translational implications. *Nat. Rev. Cancer* **11(10)**, 726–734, DOI: <https://doi.org/10.1038/nrc3130> (2011).
5. Beggs, A. D. *et al.* Whole-genome methylation analysis of benign and malignant colorectal tumours. *The J. Pathol.* **229(5)**, 697–704, DOI: <https://doi.org/10.1002/path.4132> (2013).
6. Pan, Y., Liu, G., Zhou, F., Su, B. & Li, Y. DNA methylation profiles in cancer diagnosis and therapeutics. *Clin. Exp. Medicine* **18(1)**, 1–14, DOI: <https://doi.org/10.1007/s10238-017-0467-0> (2017).
7. Bernstein, C. Epigenetic field defects in progression to cancer. *World J. Gastrointest. Oncol.* **5(3)**, 43, DOI: <https://doi.org/10.4251/wjgo.v5.i3.43> (2013).
8. Li, L. *et al.* Epigenetic inactivation of the CpG demethylase TET1 as a DNA methylation feedback loop in human cancers. *Sci. Reports* **6(1)**, DOI: <https://doi.org/10.1038/srep26591> (2016).
9. Vidal, E. *et al.* A DNA methylation map of human cancer at single base-pair resolution. *Oncogene* **36(40)**, 5648–5657, DOI: <https://doi.org/10.1038/ncr.2017.176> (2017).
10. Jin, B. & Robertson, K. D. DNA methyltransferases, DNA damage repair, and cancer. *Epigenetic Alterations Oncog.* 3–29, DOI: [https://doi.org/10.1007/978-1-4419-9967-2\\_1](https://doi.org/10.1007/978-1-4419-9967-2_1) (2012).
11. Suva, M. L., Riggi, N. & Bernstein, B. E. Epigenetic reprogramming in cancer. *Science* **339(6127)**, 1567–1570, DOI: <https://doi.org/10.1126/science.1230184> (2013).
12. Vogelstein, B. *et al.* Cancer genome landscapes. *Science* **339(6127)**, 1546–1558, DOI: <https://doi.org/10.1126/science.1235122> (2013).
13. Kantarjian, H. *et al.* Decitabine improves patient outcomes in myelodysplastic syndromes. *Cancer* **106(8)**, 1794–1803, DOI: <https://doi.org/10.1002/cncr.21792> (2006).

14. Kelly, T. K., Carvalho, D. D. & Jones, P. A. Epigenetic modifications as therapeutic targets. *Nat. Biotechnol.* **28**(10), 1069–1078, DOI: <https://doi.org/10.1038/nbt.1678> (2010).
15. Yang, X. *et al.* Gene body methylation can alter gene expression and is a therapeutic target in cancer. *Cancer Cell* **26**(4), 577–590, DOI: <https://doi.org/10.1016/j.ccr.2014.07.028> (2014).
16. Li, J. *et al.* Epigenetic targeting drugs potentiate chemotherapeutic effects in solid tumor therapy. *Sci. Reports* **7**(1), DOI: <https://doi.org/10.1038/s41598-017-04406-0> (2017).
17. Cong, L. *et al.* Multiplex genome engineering using CRISPR/Cas systems. *Science* **339**(6121), 819–823, DOI: <https://doi.org/10.1126/science.1231143> (2013).
18. The Cancer Genome Atlas Data. *Google Genomics* <https://cloud.google.com/genomics/docs/public-datasets/tcga> (2018).
19. The Cancer Genome Atlas Program. <https://www.cancer.gov/tcga> (2018).
20. Institute for Systems Biology - The Cancer Genomics Cloud. <https://shmulevich.isbscience.org/research/cancer-genomics-cloud> (2018).
21. Google Cloud. <https://cloud.google.com> (2018).
22. Google BigQuery. <https://cloud.google.com/bigquery> (2018).
23. TensorFlow. <https://www.tensorflow.org> (2018).
24. Stelzer, G. *et al.* The GeneCards suite: From gene data mining to disease genome sequence analysis. *Curr. Protoc. Bioinforma.* **54**.1.30, 1–33, DOI: <https://doi.org/10.1002/cpbi.5> (2016).
25. Hamosh, A., Scott, A., Amberger, J., Bocchini, C. & McKusick, V. Online mendelian inheritance in man (OMIM), a knowledgebase of human genes and genetic disorders. *Nucleic Acids Res.* **33**:1, D514–D517, DOI: <https://doi.org/10.1093/nar/gki033> (2005).

## Author contributions statement

M.V. conceived and conducted the research reported in this paper, and analyzed the results.

## Acknowledgements

The results attained in this research are based upon data generated by the TCGA Research Network: <https://www.cancer.gov/tcga>.

## Additional information

The author declares no competing interests.

dnn/hiddenlayer\_0/fraction\_of\_zero\_values  
tag: dnn/dnn/hiddenlayer\_0/fraction\_of\_zero\_values

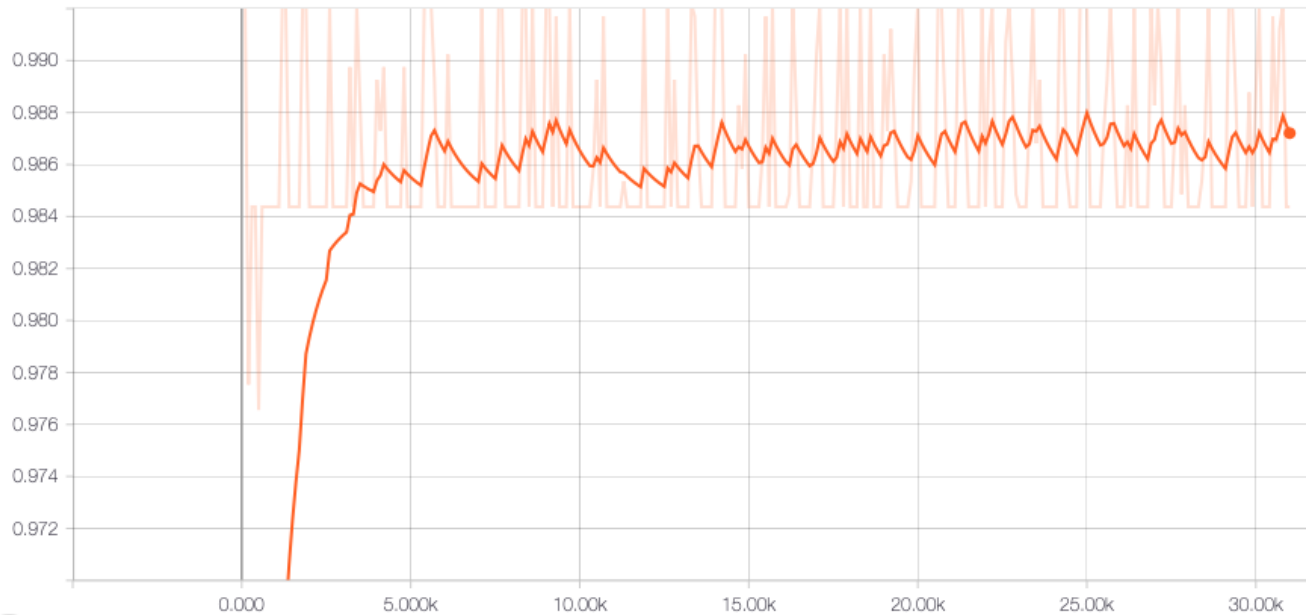


**Figure 1.** Fraction of zero weights in the classification model using methylation betas for 323,179 distinct CpG probe IDs. The horizontal axis shows the number of training steps completed by the model.

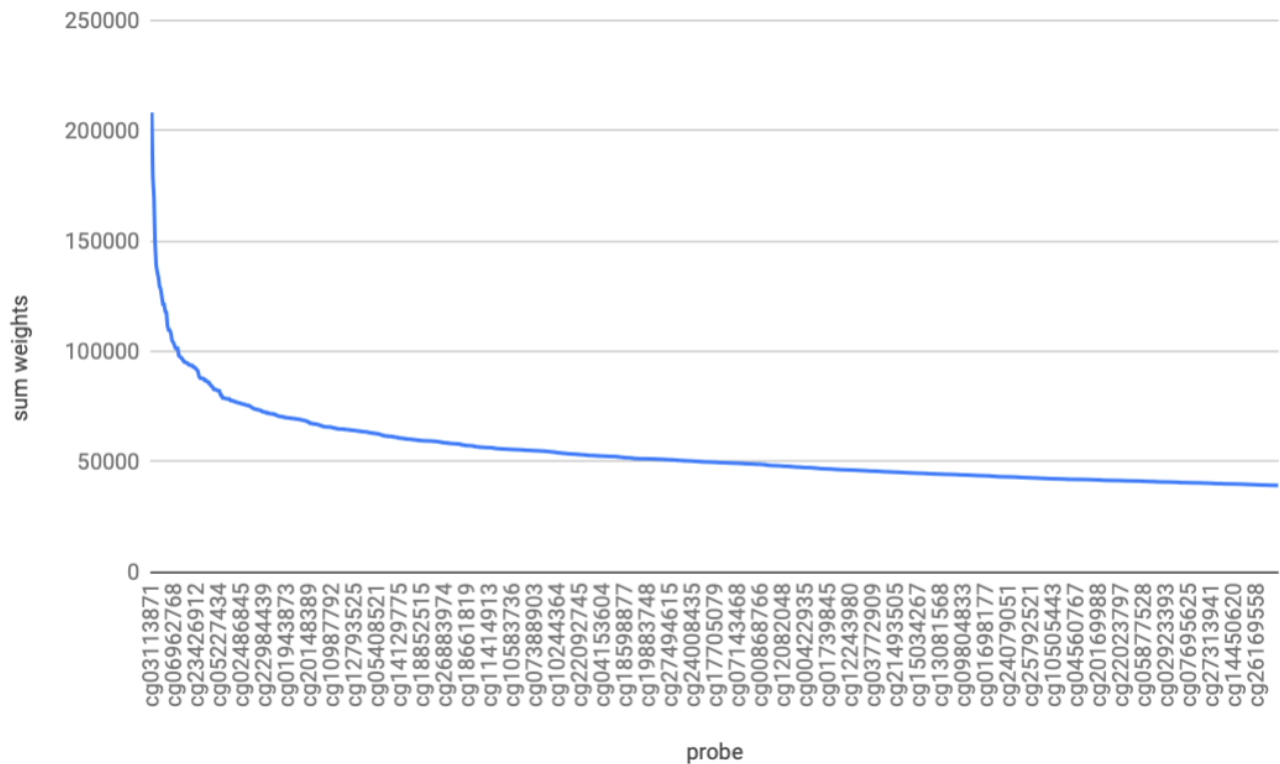


**Figure 2.** Sum of the absolute values of model weights for each CpG probe ID. The chart includes the top 1,000 probe IDs (out of 323,179 probe IDs used to train the first classification model), ordered by the sum of absolute values of weights, in descending order. The weights of the top 25 CpG sites are much higher than the weights of the remaining probes.

CpG probe ID	Chromosome	Position	Gene symbol	Function of the gene
cg24525395	chr2	60569992	N/A	To be determined.
cg14371620	chr2	118182593	AC093901.1	To be determined.
cg06282247	chr2	150425327	N/A	To be determined.
cg16171484	chr2	222425796	SGPP2	To be determined.
cg00332146	chr5	176548900	CDHR2	Involved in tumor suppression, inhibition of cell proliferation.
cg00332146	chr5	176548900	RN7SL684P	To be determined.
cg27064266	chr6	27865624	HIST1H2AL	To be determined.
cg27064266	chr6	27865624	HIST1H2BN	To be determined.
cg27064266	chr6	27865624	HIST1H2BPS2	To be determined.
cg27064266	chr6	27865624	Z98744.2	To be determined.
cg02335619	chr6	31835168	C6orf48	To be determined.
cg02335619	chr6	31835168	SNORD48	To be determined.
cg06962768	chr7	37920180	EPDR1	To be determined.
cg06962768	chr7	37920180	SFRP4	Involved in apoptosis and regulation of cell growth and differentiation.
cg00498438	chr7	66995689	SBDS	Affects apoptosis.
cg00498438	chr7	66995689	TYW1	To be determined.
cg22274662	chr7	149497004	ZNF746	To be determined.
cg13877285	chr8	26291357	PPP2R2A	Negative control of cell growth and division.
cg04693895	chr10	385155	DIP2C	To be determined.
cg12777293	chr10	7818591	TAF3	Acts as an antiapoptotic factor.
cg27139956	chr10	44974842	C10orf10	To be determined.
cg27139956	chr10	44974842	RASSF4	Tumor suppression. Promotes apoptosis and cell cycle arrest. Inhibits tumor cell growth and colony formation. Broadly expressed in normal cells, down-regulated by methylation in tumor cells.
cg13298116	chr11	62602387	EML3	To be determined.
cg13298116	chr11	62602387	MTA2	Associated with metastasis of cancer cells. Regulates gene expression. Is overexpressed in cancers. Correlates with cancer invasiveness and aggressiveness. Overexpression of MTA2 promotes metastasis of breast cancer cells. Regulates pathways involved in regulation, apoptosis, growth of normal and cancer cells.
cg14100748	chr14	90577405	TTC7B	To be determined.
cg12158535	chr14	105390913	PACS2	Involved in cell apoptosis.
cg01027010	chr16	31565018	CTD-2014E2.5	To be determined.
cg00103783	chr17	7583931	AC113189.5	To be determined.
cg00103783	chr17	7583931	MPDU1	To be determined.
cg14204735	chr17	63446943	CYB561	To be determined.
cg15751406	chr19	8823867	CTD-2529P6.3	To be determined.
cg15751406	chr19	8823867	ZNF558	To be determined.
cg09907936	chr19	58059098	ZNF135	Involved in both normal and abnormal cellular proliferation and differentiation.
cg23060618	chr21	43301197	N/A	To be determined.
cg03113871	chr22	30921800	MORC2-AS1	To be determined.
cg20180585	chr22	41381751	TEF	To be determined.

**Table 1.** Mapping of the top 25 CpG sites identified by the model to chromosome positions, genes, and respective gene functions, based on the GeneCards and OMIM databases. Nine of the genes are directly involved in the cell cycle and regulation of cell growth, differentiation, division, apoptosis, and tumor suppression. The function of the remaining genes is yet to be determined.

CpG probe ID	non-BRCA beta mean	BRCA beta mean
cg03113871	0.146	0.105
cg24525395	0.153	0.161
cg16171484	0.542	0.734
cg14100748	0.888	0.899
cg00103783	0.024	0.022
cg22274662	0.042	0.042
cg20180585	0.013	0.012
cg27139956	0.158	0.09
cg13877285	0.029	0.022
cg04693895	0.931	0.958
cg23060618	0.742	0.778
cg12158535	0.682	0.667
cg00498438	0.019	0.019
cg15751406	0.93	0.95
cg01027010	0.604	0.447
cg02335619	0.039	0.036
cg00332146	0.576	0.699
cg14204735	0.204	0.053
cg12777293	0.014	0.013
cg13298116	0.143	0.092
cg06962768	0.759	0.695
cg27064266	0.132	0.122
cg14371620	0.785	0.783
cg09907936	0.344	0.191
cg06282247	0.48	0.625

**Table 2.** Mean methylation betas for the top 25 model-selected CpG probe IDs, for the BRCA (breast cancer) and non-BRCA solid tissue samples.

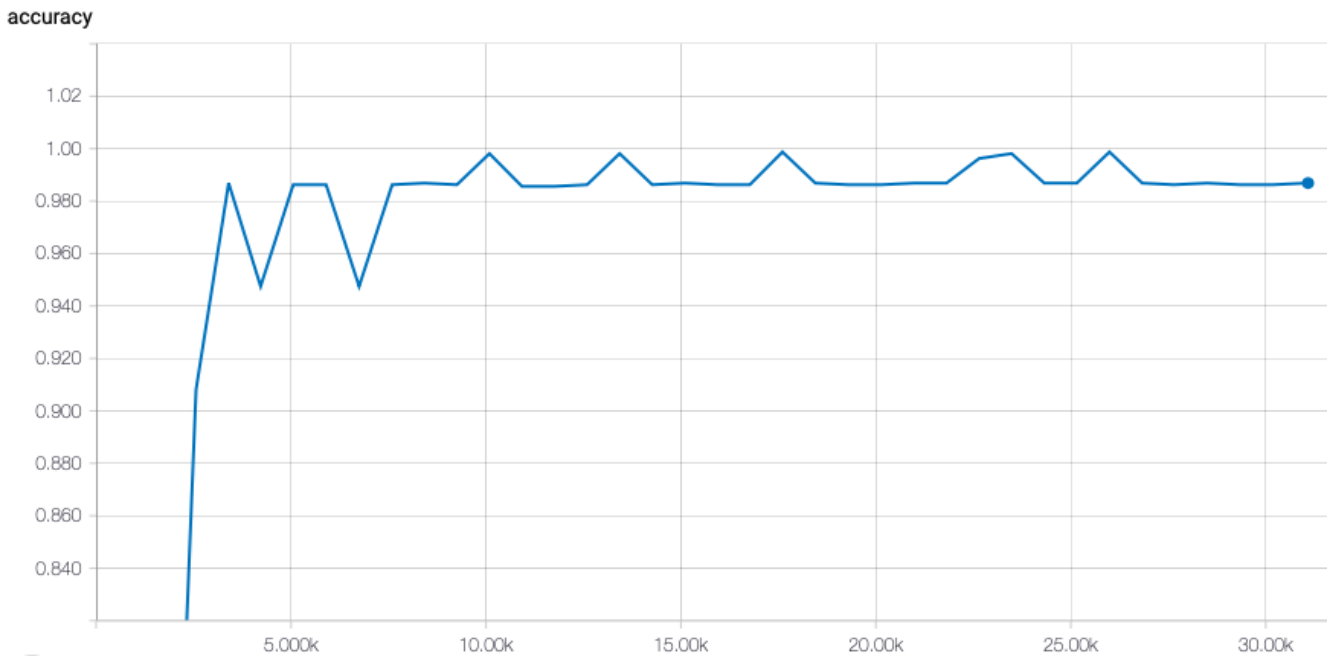


**Figure 3.** Accuracy of the classification model using methylation betas for 323,179 distinct CpG probe IDs. Accuracy was computed on the evaluation data (which was not used in training the model). The horizontal axis shows the number of training steps completed by the model. Accuracy increased during the first several thousand training steps and stabilized around 98.6%.

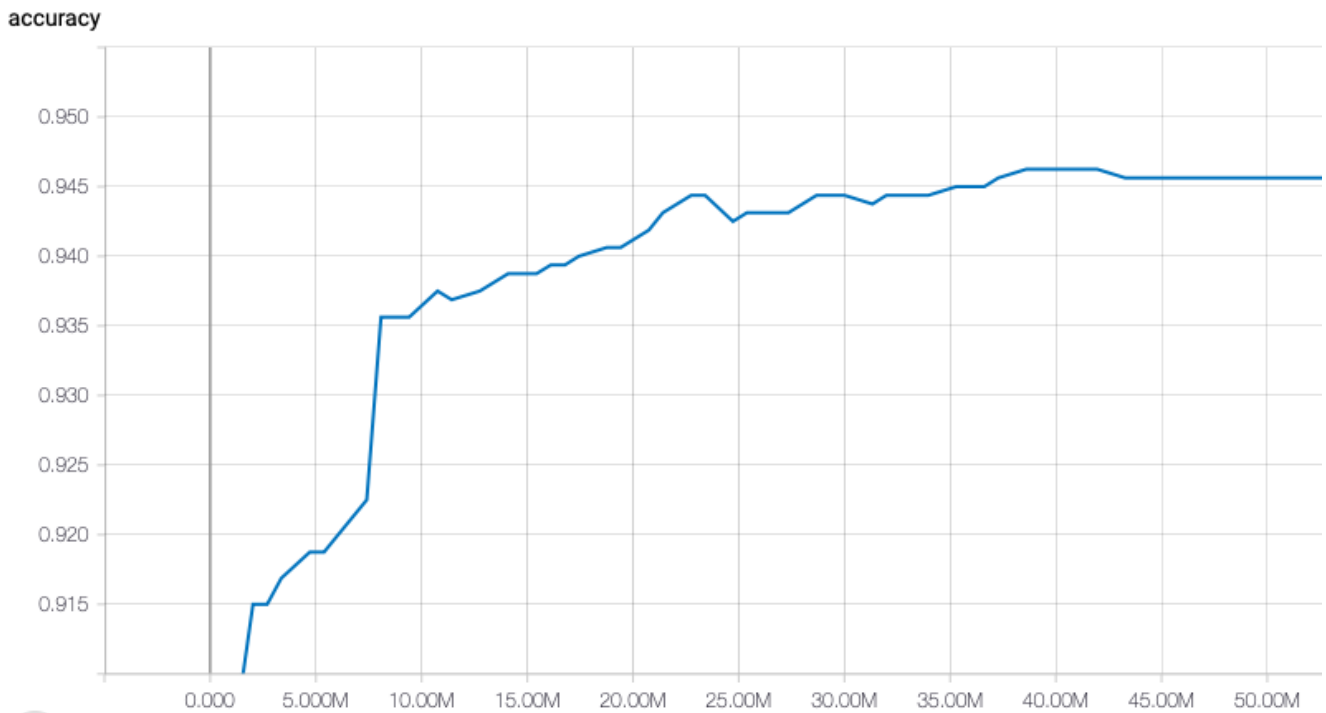


**Figure 4.** Accuracy of the second classification model trained on methylation betas of 25 CpG probes having the highest weights in the first model. Accuracy was computed on the evaluation data (which was not used in training the model). The horizontal axis shows the number of training steps completed by the model. Accuracy increased during the first forty million steps and stabilized around 94.6%.